ISSN: 0975 -8542

Journal of Global Pharma Technology

Available Online at: www.jgpt.co.in

RESEARCH ARTICLE

Synthesis, Spectral Characterization and Biological Activity of 2-[2¯ - (1-Amino -1, 5- Dinitrophenyl) azo]-Imidazole

Abd Al-Sadda HK[1]*, Al-Hussainawy MK [2], Kyhoiesh HAK[2]

1. *Department of Animal Production, College of Agriculture, Al-Muthanna University, Al-Samawah, Al-Muthanna 66001, Iraq.*
2. *Department of Chemistry, Ministry of Education, AL-Samawah, AL-Muthanna 66001, Iraq.*

***Corresponding Author: Abd Al-Sadda HK**

Abstract

The preparation and spectral identification of ligand 2-[1¯-(1-Amino- 1,5-Dinitrophenyl) azo]-Imidazole (ADNPAI) were prepared by reacting a dizonium chloride salt solution of 2,4-Dinitrophenylhydrazine with imidazole in alkaline ethanol solution. Azo dye ligand Prepared have been characterized by analytical data, Infrared, Electronic spectral data, XRD, SEM, Thermal analysis (TG-DSC-DTG), UV-Vis, and magnetic susceptibility. The biological activity azo dye ligand were tested invitro against the sensitive organisms Staphylococcus aureus (Gram-positive) and Escherichia coli, Pseudomonas aeruginosa (Gram-negative) by agar plate different technique. The activity data show appearance the ligand azo dyes prepared apparent highly active against to all the bacteria species tested.

Keywords: *Azo imidazole, ADNPAI, Thermal analysis, SEM, Antibacterial.*

Introduction

In the middle-nineteenth century all the dyes used to fabric dye that extracts from natural sources. The first dye that was used and synthesized in 1856 by William Perkin .The first commercially azo dye was Bismarck brown [1]. Azo dyes acquired a wide interest in applying to biological system and indicator in complex metric titration of analytical chemistry [2, 3].

Aromatic azo compounds especially are used as acid-base indicators, also used in biological strains and commercial colorants for clothing, plastics [4]. Colour changes are caused by change in extent of the delocalization of electrons. More delocalization shifts the absorption max to longer wavelengths and makes the light absorbed redder, while less delocalization shifts the absorption max to shorter wavelengths [5].

Some of the azo dyes amide antibacterial drugs were the first effective chemotherapeutic agents that could be used systemically for the cure of bacterial infection in humans. A series of azo dyes containing the sulfonamide and NH group functional group were synthesized as potential antimicrobial agents [6]. Metallic azo compounds might be divided into two categories, named the also groups were involved by bonding. The former could be derived to also compounds that had donor groups (OH, COOH, NH_2, SH) a congenial position to produce 5 and 6 metallic membered compounds [7].

Experimental

Chemicals and Methods

All chemicals and solvents were highest purity obtained from B.D.H, Sigma-Aldrich, Merck, Scharlan and Fluka. Imidazoles were purchased from Aldrich chemical company and all analytical grade chemicals were used without further purification. Mannitol salt agar and Nutrient broth are used to grow bacteria from al Muthanna university labs.

All other organic chemical solvents and 2, 4-Dinitrophenylhydrazine was available from multiple companies, Fluke, B.D.H, Sigma-Aldrich. The solvents were supplied by BDH chemicals Ltd pool England. These are Methanol, Ethanol, DMSO, and Acetone. The melting points of the azo dye ligand were

taken in an open capillary tube which was uncorrected by using electro thermal 9300. FTIR spectra were taken on Shimadzu 8400 δ FTIR spectrometer in KBr pellets (cm^{-1}). Electronic spectra were recorded using T 80-PG UV- visible spectrophotometer in absolute ethanol (10^{-3}M) in the range (200-1100) nm.

Elemental analyses (C.H.N) were estimated out on a micro analytical unit of EA 300 C.H.N Element Analyzer. X-ray diffraction was taken on Bestec Germany Aluminum anode model X-Petro, wavelength of X-ray beam (Cu kα) 1.54A°, and material=Cu, the Voltage = 40KV and current = 30mA. Scanning electron microscopy (SEM) images of azo dye ligand and its metal complexes were taken using micrograph ZEISS EM3200. The pH solutions were measured with a Philips PW 9421 pH meter (± 0. 001).

Synthesis of Heterocyclic Azo Dye Ligand (ADNPAI)

The new heterocyclic azo dye ligand (ADNPAI) was prepared in reaction by flowing methods proposed by Al-Adilee et al [8] with some modification (Figure 1). A diazonium solution was prepared by dissolving 1.98 g (0.01mol) of 2, 4-Dinitrophenylhydrazine in 40 mL of distilled water and 4 mL of concentrated hydrochloric acid. The filtered solution was cooled to (0-2) °C. To this mixture a solution of 0.8 g (0.01mol) sodium nitrite in 30 mL distilled water was added dropwise at (0-5) °C and stirred for 25 min.

The resulting diazonium chloride solution was added dropwise with cooling and stirring continuously at (0-2) °C into a 500 mL beaker containing 0.75 g (0.01 mol) of imidazole was dissolved in 50 mL of ethanol and 15 mL of 5% sodium hydroxide for coupling after the mixture had been stirring for two hours at (0-2) °C in an ice - bath, it was acidified with dilute hydrochloric acid to pH= 6.0.

The crude product was separated by filtration, washed with distilled water and dried. The ligand (ADNPAI) obtained were finally dried in oven at 70°C for several hours and keep in a desiccators under desiccators over anhydrous. The purity of the azo dye was determined by thin layer chromatography TLC.

The yield of the reaction was 77% and its colour was dark yellow crystals and m.p = 106°C. The molecular structure of azo dye ligand (ADNPAI) was elucidated by C.H.N.S, X-ray, TGA-DTG-DSC, FTIR and UV- Visible spectra. The following chart illustrates the method of preparation azo dye ligand 2-[2 (1- Amino -1, 5- Dinitrophenyl) azo]-imidazole, (ADNPAI). The m.p, yield, molecular formal, M. wt, colour and element analysis data (C.H.N.S) of the Imidazole dye ligand (ADNPAI) collected in (Table 1).

Table 1: Analytical and Physical data of Imidazole dye ligand (ADNPAI)

Compound	Color	Optimal pH	m.p C°	Yield %	Molecular formula (Mole .W.t)	Found (Calc.)%				
						C	H	N	S	M
ADNPAI = HL	Dark yellow	6	106	77	$C_9H_7N_7O_4$ (277.20)	(39.00) 38.82	(2.55) 2.60	(35.37) 35.41	(0) 0.001	---

Ligand= (ADNPAI) = HL

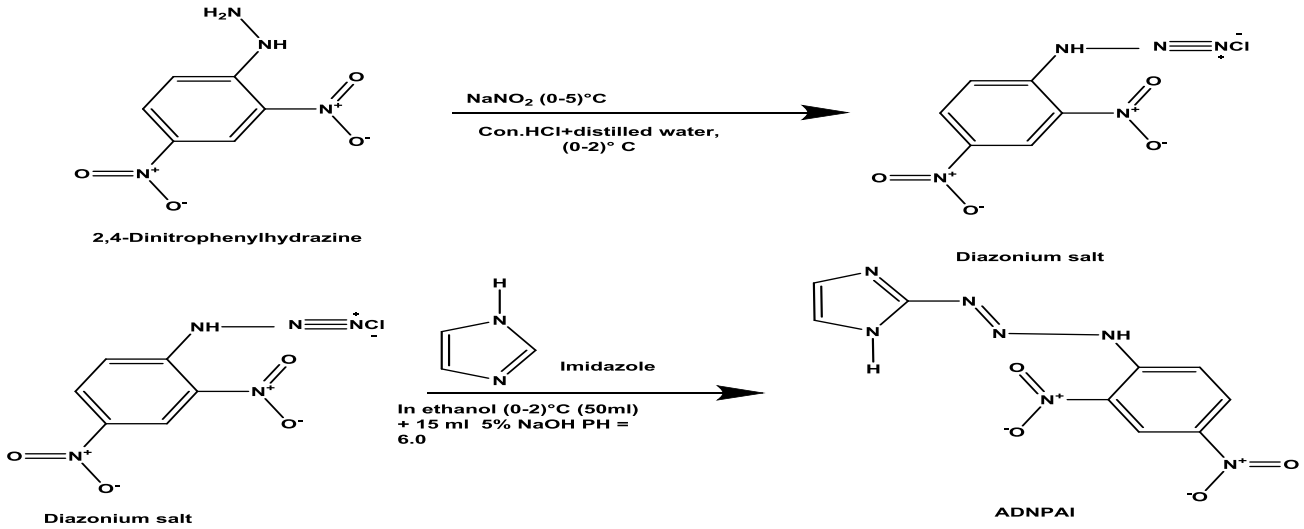

Fig. 1: Synthesis of heterocyclic azo dye ligand (ADNPAI)

Biological Experiments

Biological Study

In this study, the inhibitory biological efficacy of the compound prepared in this study was tested on two different types of Gram-positive, negative bacteria using the sensitivity test method.

Biochemical Test of Bacteria

Staphylococcus aureus and Escherichia coli, Pseudomonas aeruginosa were as test bacteria, Nutrient broth and MS (mannitol salt) agars were used for the isolation, cultivation and differentiation of Escherichia coli, Pseudomonas aeroginosa and Staphylococcus aureus respectively. The diagnosis of bacteria was also carried out by using the microscope method (Gram's Method) [9]. The petri dishes were incubated at (37°C) for (24 hr).

Result and Discussion

Characterization of Azo Dye Ligand (ADNPAI)

The azo dye ligand (ADNPAI) was dark yellow crystals. The azo dye ligands were stable at room temperature and soluble in most organic solvents such as methanol, ethanol, acetone, DMF and DMSO, but insoluble in water. The experimental result of the elemental analysis of the prepared azo dye ligand (ADNPAI) is in good agreement with theoretical expectations.

Electronic Spectral Studies

In unsaturated system, pi-electrons predominantly determine the state of electron sheath, which are excited by the absorption of uv/vis-light. There are unshared electrons in molecules like nitrogen; oxygen, etc. are usually called n-electrons. Non-bonding electrons are boundless strongly than the bonding electrons. Typical electronic spectra in organic compounds are $\pi \rightarrow \pi^*$ and $n \rightarrow \pi^*$transitions. The $\pi \rightarrow \pi^*$ transition is very intense (allowed) or weak (forbidden).

But the $n \rightarrow \pi^*$transition is generally forbidden and weak intensity. Azo compounds exhibits $n \rightarrow \pi^*$ transition characteristics of the N=N group, the intensity of the band depends on stereochemistry of nitrogen-nitrogen linkage of straight chain compounds containing nitrogen-nitrogen bond gives rise to a low intensity band in the near UV-visible-region [10]. The solvent effect on spectra, resulting from electronic transitions, is primarily dependent on the chromospheres and the nature of transition ($\sigma \rightarrow \sigma^*, n \rightarrow \sigma^*, n \rightarrow \pi^*, \pi \rightarrow \pi$) and charge transfer (CT) absorption. The electronic transitions of particular interest in this respect are$n \rightarrow \pi^*$, $\pi \rightarrow \pi$ transfer (CT) absorptions [11].

Organic molecules composed of directly attached electron donor and electron acceptor moieties have received considerable attention as possible models for a number of photochemical and photo biological processes. Excitation of such molecules induces transfer of an electron from donor to acceptor and is often accompanied by rotational relaxation to a twisted conformation of the donor relative to the acceptor, forming the so-called Twisted Intra molecular Charge Transfer (TICT) state [12].

Molecules of the type D- π -A where the donor and acceptor groups are connected to the ends of a conjugated system exhibit large changes in dipole moment ($\Delta\mu$) up on excitation due to photo induced Intra molecular charge transfer process. The extent of charge transfer depends on the nature of the donor (D) and acceptor (A) groups and the length of the π system. Conformational dynamics of the D and A fragments can also significantly influence the photochemistry of such systems.

The π^* scale is based on the solvent induced shift of the longest wavelength $\pi \rightarrow \pi^*$ absorption band is indicator of the type D- π -A [13]. The electronic absorption spectra of the (ADNPAI) were recorded in freshly ethanol solution (10^{-3}M) at room temperature. The spectral data of the azo dye ligand (ADNPAI) are summarized in Table 2. The electronic spectrum of free ligand is characterized by two absorption is banded in U.V-Visible.

These bands appear at the position 229 nm (43668cm^{-1}) and 363 nm (38022 cm^{-1}). The first band can be attributed to a $\pi \rightarrow \pi^*$ transition within the imidazole ring. While the second band is due to $n \rightarrow \pi^*$ transition resulted from the presence of the group containing double bond, in addition to the presence of hetero atom carrying an ion pair

of electrons such as (=C=N-) in the imidazole ring in addition to intermolecular charge-transfer taken place from the phenyl ring to the imidazole ring through the azo group (-N=N-), this band showed at a red shift on coordination with a metal ions [8,14], The UV-visible spectra of azo dye ligand (ADNPAI) are shown in (Figure 2) and Table 2. Solvents effect the wavelength and intensity of absorption bands are both affected when a molecule is in solvent environment. This is due to unequal perturbation of the ground and exited electronic state of the molecule, which depends on the nature of the solute-solvent interactions [15]. The interpretation of solvent effect is often made difficult, because they are small and not easy to measure precisely and also because several individual effects, superimposed on one another, contribute to the observed changes [10, 16, 17].The dipole moment difference between exits state and ground state indicates the solvent effect on solvatochromic shift. A series of absorption spectra of (ADNPAI) were recorded in Ethanol, DMSO, THF, DMF and Acetone solutions in the electronic states of the compound (Figure 3).

Table 2: The spectral data of the azo dye ligand (ADNPAI)

Compound	λ_{max} (nm)	Absorption bands(cm^{-1})	Transitions
Ligand=HL (ADNAPI)	363	38022	n →π*
	229	43668	π →π*

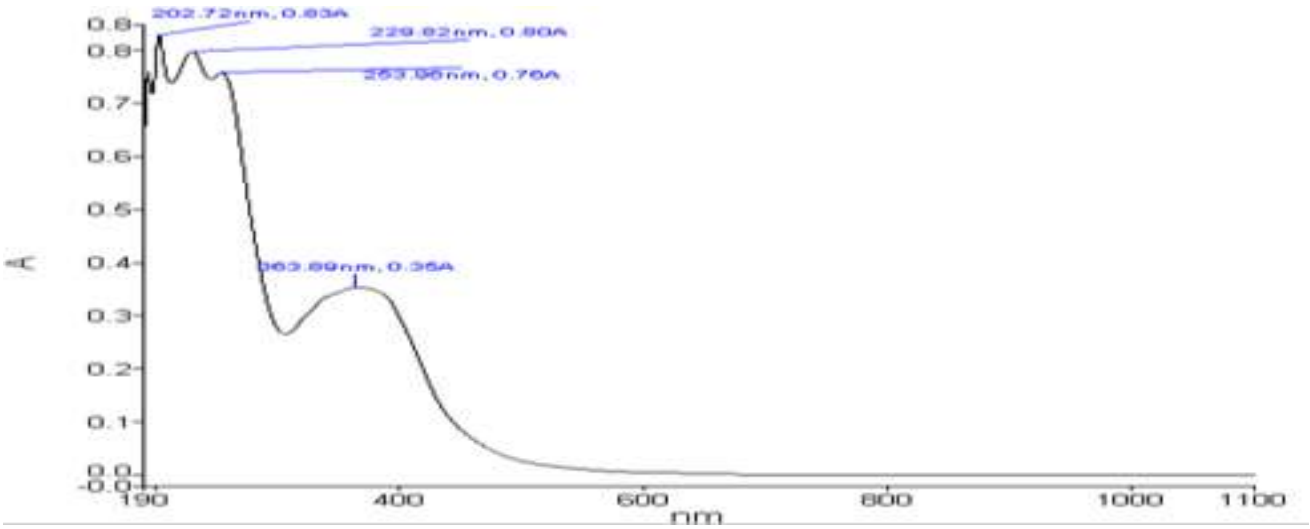

Fig. 2: UV. Visible spectrum of azo dye ligand (ADNPAI)

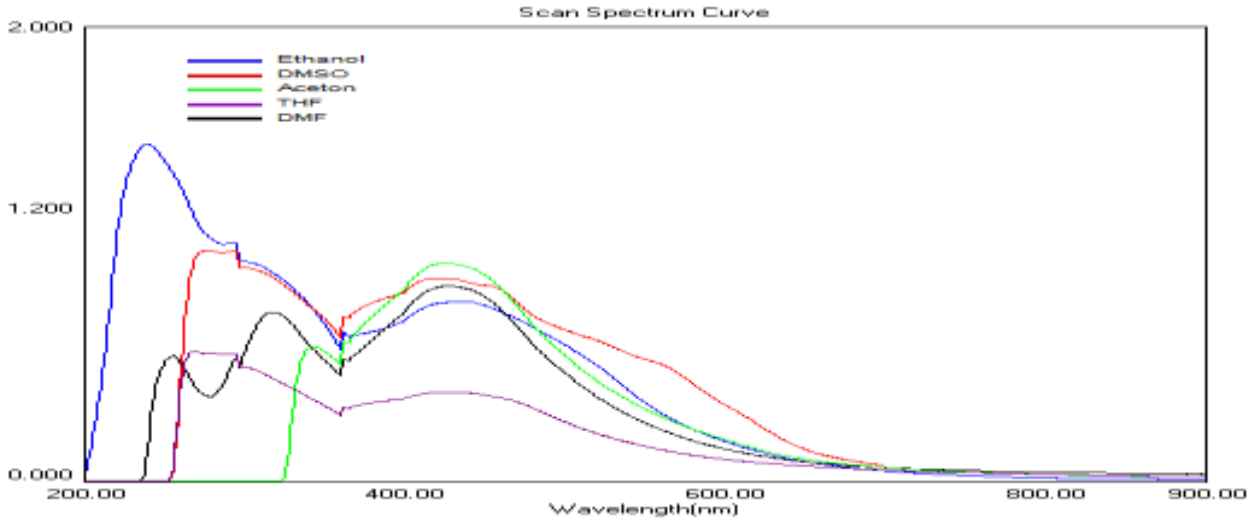

Fig. 3: Electronic absorption spectra of azo dyes at room temperature DMSO, DMF, THF, EtOH and Acetone

Infrared Spectra

Infrared spectral data of the prepared azo dye ligand (ADNPAI) (Table 3).The IR spectrum of the ligand showed a strong band at 3325 cm^{-1} assignable to the υ(NH) of the imidazole ring [18-20]. The band remains in the same region in the free ligand.

The spectrum of free ligand shows two weak bands at 3088 cm^{-1} and 2920 cm^{-1} due to υ(C-H) aromatic and aliphatic respectively. The medium band observed at 1519 cm^{-1} in the free ligand was attributed to υ (C=N) stretch of the azomethine. A medium intensity band at 1413 cm^{-1} in the free ligand was attributed to υ (N=N) stretch of the azo group. A group of bands located at 1109 cm^{-1}, 831 cm^{-1}, 823 cm^{-1} and 740 cm^{-1} assigned to the Benz. R. Deff. and Im. R. Deff. Frequency respectively .

Depend on IR spectral data lead to suggest that azo dye ligand (ADNPAI) behaves as a trident chelating agent coordinating with metal ions by a phenolic oxygen, azo nitrogen which is the farthest of imidazole ring and nitrogen atom in the imidazole ring to forming two five membered chelating ring, The infrared spectra of azo dye ligand are shown in (Figure 4).According to these results the structure of these metal complexes may be proposed in (Figure 5), shown below.

Table 3: Characteristic IR absorption bands of the ligand (ADNPAI) in cm^{-1} units (KBr disc)

Group	*Ligand*
υ (C-H) aromatic	**3088 m.**
υ (NH)	**3325 s.**
υ (C=N)	**1627 s. br.**
υ (N=N)	**1413 w.**
υ(C-N=N-C)	**1222 m.**
υ(Benz. R. Deff.)	**1109 w. 831 w.**
υ(Imi- R. Deff.)	**823 s. 740 m.**
υ (C-N=N-C)	**630 w.**

HL=ligand (ADNPAI), Vs = very strong, s = strong, m= medium, w = weak, sh = sholder, br =broad

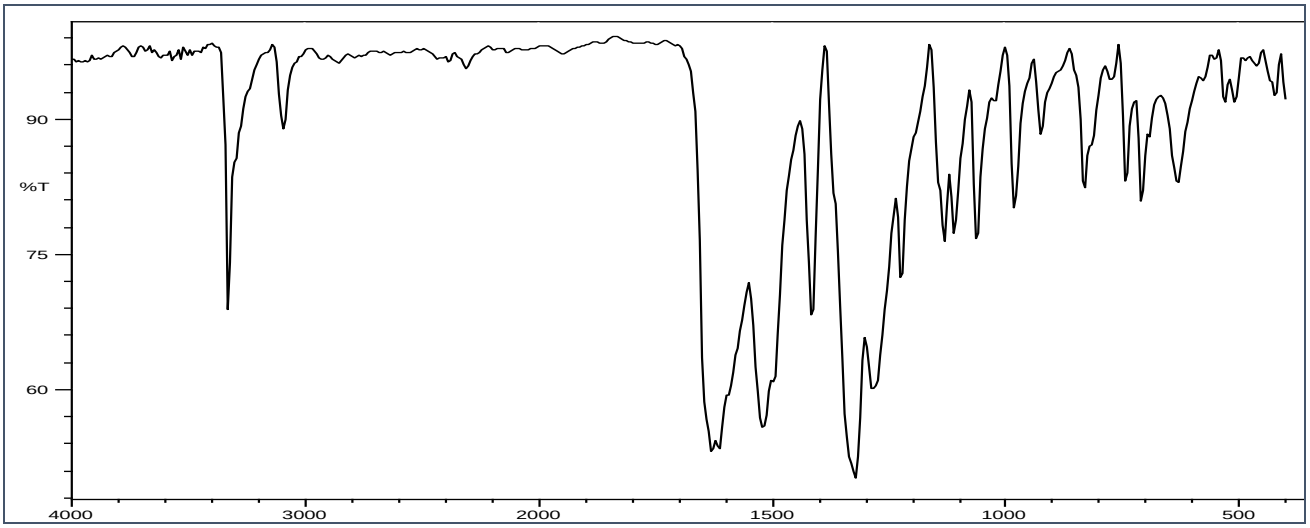

Fig. 4: IR Spectrum of azo dye ligand (ADNPAI)

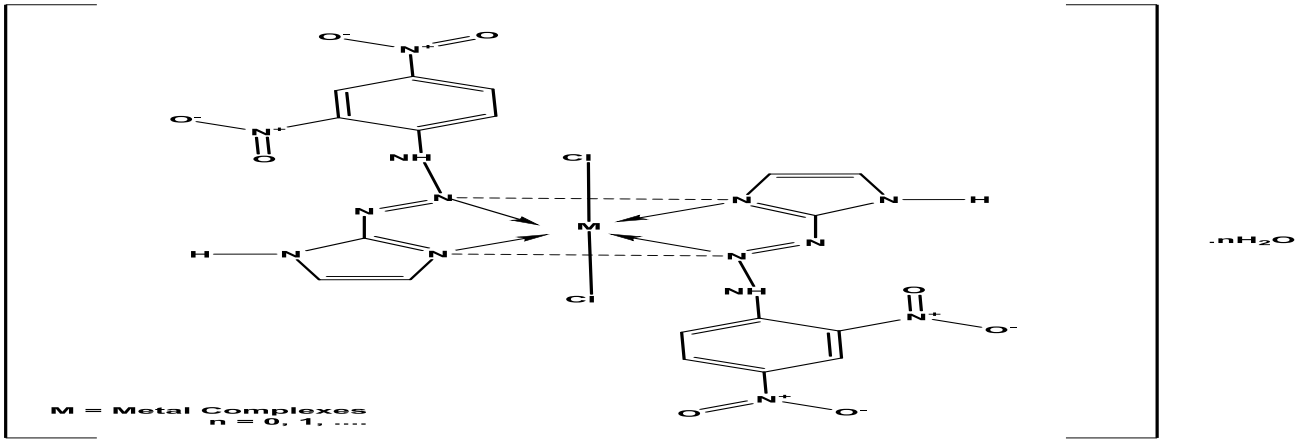

Fig. 5: The proposed chemical formula of chalet complexes

Thermal Analyses

The thermo gravimetric analysis (TGA), differential thermo gravimetric decomposition (DTG) and differential scanning calorimetry (DSC) curves for the ligand are presented in (Figure 6).The results of thermo gravimetric analyses of ligand (ADNPAI) are given in (Table 4). The thermo grams have been carried out in the range 22-800 °C at a heating rate of 10 °C min^{-1} in oxygen atmosphere.

The TGA curve reveals the ligand of the formula ($C_9H_7N_7O_4$) show four stages of decomposition. The first stage within the temperature range of 22-161°C is related to the moisture and volatile substances such as evolution of CO_2 gas, these stages involved mass losses of 3.3 %. The second decomposition stage within the temperature range of 161-318 °C corresponds to the loss of azo group, these stages involved mass losses of 21.3 %. The third decomposition stage within the temperature range of 318-465°C corresponds to the loss of imidazole ring, these stages involved mass losses of 34.0 %.

The final decomposition stages in the temperature range of 465-570 °C correspond to the loss of further complete decomposition of a part of the ligand, these stages involved mass losses of 83.7 %. The DSC curve shows endothermic peaks at 310, 511 °C leaving carbon as residue [8, 21, 25].

Table 4: Thermoanalytical results (TG, DTG, DSC) of ligand and metal complex

Compound	TG Range (°C)	DTG Max (°C)	Mass loss%	Assignment	Residue	DSC(°C)
(ADNPAI)=HL $C_9H_7N_7O_4$	22-161 161-318 318-465 465-570	220 310 500	3.3 21.3 34.0 83.7	Evolution of Co_2 and moisture Loss Azo group Loss Imidazole Ring, Loss of a part of the ligand	_	310 (+) 511 (+)

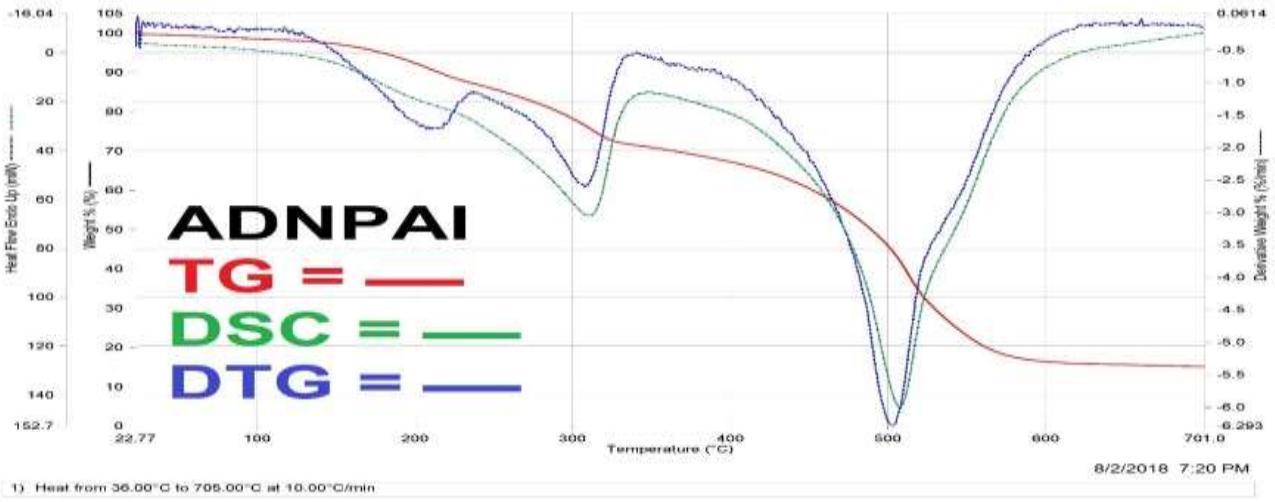

Fig. 6: TG-DTG-DSC curves of ligand (ADNPAI)

X-Ray Diffraction Study (XRD)

The (XRD) of ligand (HL) were recorded in the range of 2Θ = (0-80)° value, The (XRD) patterns of ligand are shown in (Figure 6), Broad peak and sharp peak for ligand (HL) was observed indicating they indicate the poly crystalline nature. Given the spectrum of X-ray diffraction patterns ligand sharp peaks, as it is an indicated crystalline nature structure a result of the micro-strains and cracking crystalline faulting result of the distortions of the crystal and domain size of the crystal and distribution of domain size [8, 26, 27].

To calculate d-spacing of reflections were obtained using Bragg's equation (1) [8, 28].

$$n\lambda = 2d\sin\theta \quad (1)$$

Where d is the spacing between the crystalline levels, n is an integer (1, 2, 3...), λ is the wavelength of X-ray CuKα = 1.540598 A°, Θ is the diffraction angle. The values of d and associated data depict the 2Θ value of each peak, relative intensity for ligand are listed in (Table 5). The results show that ligand (HL) had 10 reflections with maxima 2Θ = 32.80° corresponding to d value 2.71 A° indicates the crystalline state.

The average size of the particles and their size distribution were evaluated by the Scherer equation (2) [29].

$$D = k\lambda/\beta Cos\theta \quad (2)$$

Where D is the average grain size, k is Blank's constant (0.891), λ is the X-ray wavelength (0.15405 nm), and Θ and ß are the diffraction angle and full width at half maximum of an observed peak, respectively [28, 30]. The average size of the particles for ligand (ADNPAI) was calculated and was found to be 23.10, 26.81, 31.88, 32.80, 45.56, 46.92, 56.48, 58.39, 75.36 nm, respectively. Well been calculated dislocation density (δ) through the following relationship (Eq. 3) [26, 30].

$$\delta = 1/D^2 \quad (3)$$

Where δ is dislocation density, D is the average grain size. The particle size distribution histogram of the ligand (ADNPAI) was presented in (Figure 7) and (Table 5).

Table 5: Crystallographic data for ligand (ADNPAI)

Compound	°2Θ(degree)	d Spacing (A°)	FWHM [°2Θ]	Crystallite Size D(nm)	Lattice Strain	Dislocation density δX (nm)²	Intensity I/I₀) %(
ADNPAI = HL	23.10	3.83	0.35	23.90	0.0075	0.00173	38
	26.81	3.31	0.17	48.18	0.0031	0.00043	39
	31.88	2.80	0.18	48.73	0.0027	0.00042	54
	32.80	2.71	0.17	48.86	0.0025	0.00041	100
	45.56	1.97	0.19	45.60	0.0017	0.00049	28
	46.92	1.92	0.70	12.80	0.0072	0.00613	16
	56.48	1.61	0.71	13.30	0.0056	0.00563	14
	58.39	1.56	0.23	40.26	0.0019	0.000618	18
	75.36	1.27	0.86	12.17	0.0050	0.006774	10

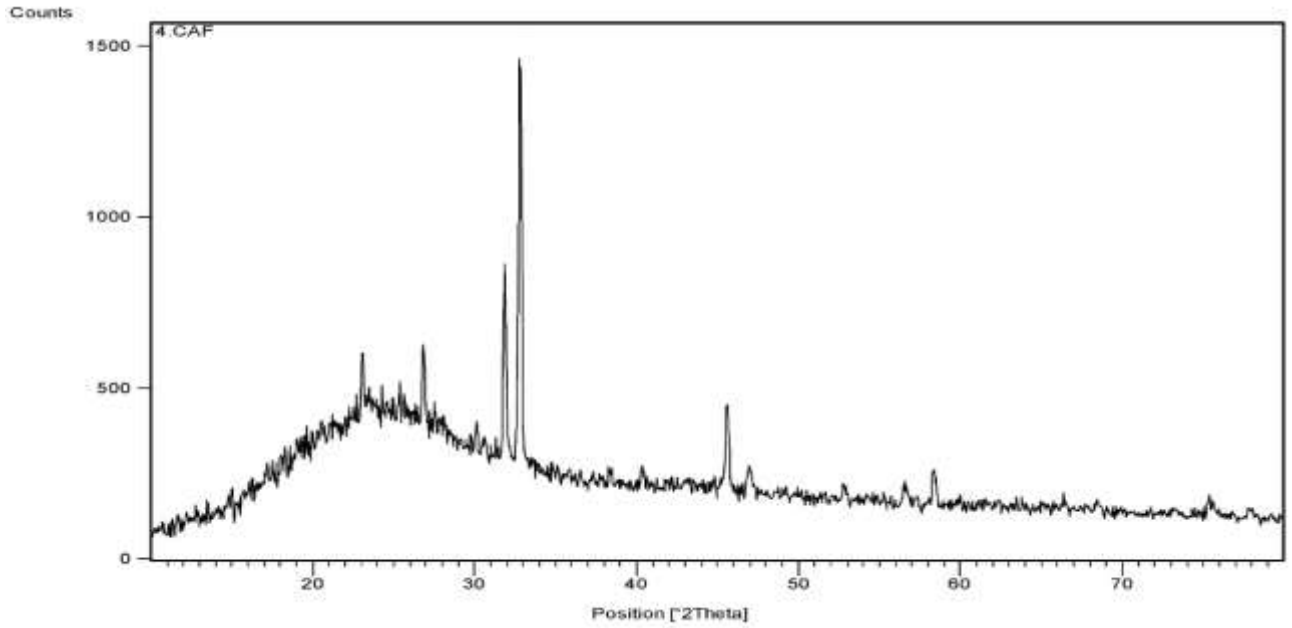

Fig. 7: XRD patterns of ligand (ADNPAI)

SEM Analysis

Scanning electron microscopy (SEM) of the ligand studies the surface morphology and shape of the particles and aggregation, in addition to the distribution of these particles. The scanning electron microscope technique was adopted at a cross-sectional distance of 1µm and a magnification force of Mag = 20.00 K X. The SEM image of ligand has been illustrated in (Figure 7).

SEM image shows the ligand (ADNPAI) have formed of peripheral spherical shape with average size 95 nm with a ratio of less than aggregation. The SEM showed that the particles are agglomerated and non-uniform particles are observed in some cases.

Moreover, SEM micrographs of the ligand (ADNPAI) revealed that the surface morphology of ligand [30, 35].

The calculations of particle size were performed using MagniSci software (Figure 8).

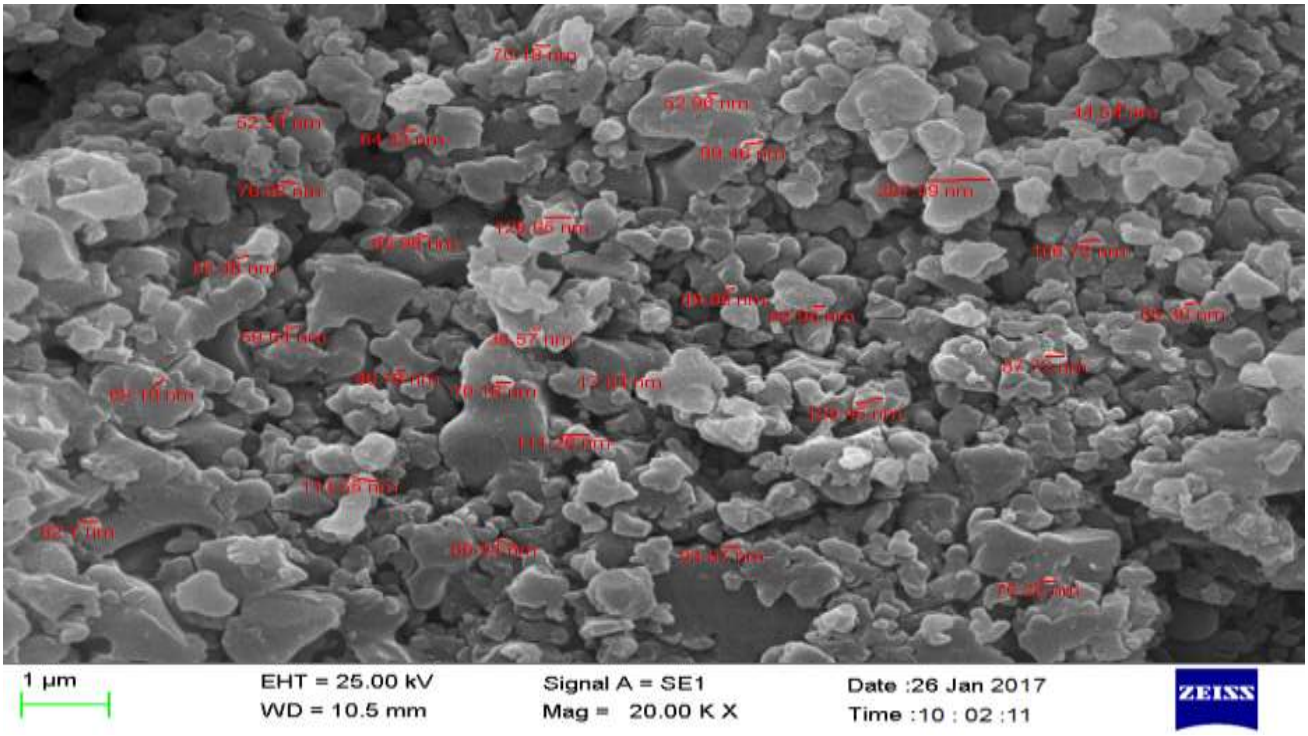

Fig. 8: SEM images of ligand (ADNPAI)

Biological Activity

This study involved effect of three types from negative bacteria (Escherichia coli, Pseudomonas aeruginosa) and (Staphylococcus aureus) on ligand. These bacteria have been chosen because of their importance in the medical field, as they cause a number of diseases, and they differ in the nature of their resistance to antibiotics and therapeutic chemicals [36, 38].

The results shown of the efficacy test for the tested compound ADNPAI were in the tables have an inhibitory effect on the three types of bacteria that is used by using spots diffusion method, The tested ligand show a remarkable antibacterial activity against tested bacteria (Table 6).

The bacteria Pseudomonas aeruginosa was of a high activity and sensitivity towards ligand also the results showed that the type of the compensated groups in the prepared compound affect the degree of effectiveness and the type of bacteria affecting them, such as the group of (-N=N- , NO and NH), that is found in the tested ligand [9,39,40].

Conclusions

We have prepared and structurally characterized azo dye ligand (ADNPAI) derived from imidazole. The formation of the ligand and has been confirmed by the analytical data (C.H.N), IR, electronic spectra. The azo dye ligand have different morphologies as appeared in XRD and SEM, TGA of ligand was also studied and gave good result in thermal stability.

The azo ligand (ADNPAI) behaves as a bidentate chelating agent coordination throughout the N_3 atom of the imidazole ring and another nitrogen atom of azo group to form five-member metal rings. The geometry is proposed for all complexes octahedral stereochemistry. On the basis of their analytical and spectral data, we propose octahedral geometry for all metal complexes.

The ligands and their chelates are subjected to thermal analysis. The biological activity of the synthesized ligands and they showed remarkable biological activity. The study appears strong Biological efficiency of ligand that is tested against Escherichia coli, Pseudomonas aeruginosa and Staphylococcus aureus.

Acknowledgments

The author is very grateful to Dr. Khalid Al-Adilee for assistance in the preparation of the manuscript.

References

1. Jetter J W (2010) Book Review of Organic Chemistry. Marc Loudon Roberts: Norristown, 584-586.
2. Hunger K (2003) Industrial Dyes Chemistry properties Applications. Weinheim: Wiley., 978-3-527.
3. Golka K, Kopps S, Myslak Z W (2003) Carcinogenicity of azo colorants: influence of solubility and bioavailability. Toxicol. Lett., 151(1): 203-210.
4. Zollinger H (1987) Color chemistry synthesis, properties and Application of organic dyes and pigment. VCH Publishers, New York, 92-102.
5. Cao X, Wang H, Zhang S, Nishimura O, Li X (2018) Azo dye degradation pathway and bacterial community structure in biofilm electrode reactors. Chemosphere, 219-225.
6. Wilson and Gisvolds (2004) Textbook of organic medicinal and pharmaceutical chemistry. Lippincott: USA, 269.
7. Ziarani G M, Moradi R, Lashgari N, Kruger H G (2018) Metal-Free Synthetic Organic Dyes, 47-93.
8. Al-Adilee K, Kyhoiesh H A (2018) Preparation and identification of some metal complexes with new heterocyclic azo dye ligand 2-[2- - (1-Hydroxy -4- Chloro phenyl) azo]- imidazole and their spectral and thermal studies. J. Mol. Struct., 1137: 160-178.
9. Gram C (1884) Über die isolierte Färbung der Schizomyceten in Schnitt- und Trockenpräparaten. In Fortschritte der Medizin, 2: 185-189.
10. Burgess C (2017) The Basis for Good Spectrophotometric UV–Visible Measurements. UV-Visible Spectrophotometry of Water and Wastewater, 1-35.
11. Karoui R (2018) Spectroscopic Technique: Fluorescence and Ultraviolet-Visible (UV-Vis) Spectroscopies. Mod. Tech. for Food Authentication, 219-252.
12. Sridevi Venkatachalam (2016) Spectroscopy of Polymer Nanocomposites, India, 130-157.
13. Ding CC, Wu S Y, Xu Y Q, Wu L N, Zhang L J (2018) DFT studies for three Cu(II) coordination polymers: Geometrical and electronic structures, g factors and UV-visible spectra. Chem. Phys., 508: 20-25.
14. Kobayashi T, Yabushita A, Kida Y (2018) Development of Sub-10 fs Visible-NIR, UV, and DUV Pulses and Their Applications to Ultrafast Spectroscopy. Front. Adv. Mol. Spectrosc., 287-306.
15. Figgis B N (1960) Modern Coordination Chemistry, Interscince: Lewis, New York, 123-144.
16. Nasri S, Brahmi J, Turowska-Tyrk I, Schulz C E , Nasri H (2017) Synthesis, UV-visible and Mössbauer spectroscopic studies and molecular structure of the low-spin iron(II) Bis(tert - butyl isocyanide)(5, 10, 15, 20-[4-(benzoyloxy)phenyl]porphyrin) coordination compound. J. Organomet. Chem., 846: 176-184.
17. Edwards AA, Alexander BD (2017) UV-Visible Absorption Spectroscopy, Organic Applications. Encyclop. Spectrosc. Spectromet., 511-519.
18. Iramain M A, Davies L, Brandán S A (2018) FT-IR, FT-Raman and UV–visible spectra of potassium 3-furoyltrifluoroborate salt. J. Mol. Struct., 1158: 245–254.
19. Morzyk-Ociepa B, Szmigiel K, Turowska-Tyrk I, Malik-Gajewska M, Banach J, Wietrzyk J (2018) New mono- and dinuclear complexes of 7-azaindole-3-carboxaldehyde with palladium (II): crystal structure, IR and Raman spectra, DFT calculations and in vitro anti-proliferative activity. Polyhedron, 153: 88-98.
20. Belova NV, Sliznev VV, Christen D (2017) Infrared and Raman spectra of tris(dipivaloylmethanato) lanthanides, Ln(thd)3 (Ln = La, Nd, Eu, Gd, Tb, Ho, Er, Tm, Yb, Lu). J. Mol. Struct., 1132: 34-43.
21. Do Nascimento A C S, Caires F J, Colman T A D, Gomes D J C, Bannach G, Ionashiro M (2015) Thermal study and characterization of nicotinates of some alkaline earth metals using TG-DSC-FTIR and DSC-system photo visual. Thermochim. Acta, 604: 7-15.
22. Nascimento A L C S, Parkes G M B, Ashton G P, Fernandes R P, Teixeira J A, Nunes W D G, Caires F J (2018) Thermal analysis in oxidative and pyrolysis conditions of alkaline earth metals picolinates using the techniques: TG-DSC, DSC, MWTA, HSM and EGA (TG-DSC-FTIR and HSM-MS). J. Anal. Appl. Pyrolysis., 67-75.
23. Müsellim E, Tahir M H, Ahmad M S, Ceylan S (2018) Thermokinetic and TG/DSC-FTIR study of pea waste biomass pyrolysis. Appl. Therm. Eng., 137: 54-61.
24. Colman M D, Lazzarotto S R da S, Lazzarotto M, Hansel F A, Colman T A D (2016) Schnitzler, E. Evolved gas analysis (TG-DSC-FTIR) and (Pyr-GC-MS) in the disposal of medicines (aceclofenac). J. Anal. Appl. Pyrolysis, 119: 157-161.
25. Sun R, Zhao M, Zhuang D, Li X, Gong Q, Ouyang LCao M, (2016) Cu2Zn SnS4 ceramic target: Determination of sintering temperature by TG–DSC. Ceram. Int., 9630-9635.

26. Hussain G, Abass A, Shabir G, Athar A, Saeed A, Saleem R, Ali F, AinKhan M (2017) New acid dyes and their metal complexes based on substituted phenols for leather: Synthesis, characterization and optical studies, J. Appl. Res. Technol. 15: 346-355.

27. Tiamiyu A A, Odeshi A G, Szpunar J A (2018) Characterization of coarse and ultrafine-grained austenitic stainless steel subjected to dynamic impact load: XRD, SEM, TEM and EBSD analyses. Materialia 1-46.

28. Caglar Y, Caglar M, Ilican S (2018) XRD, SEM, XPS studies of Sb doped ZnO films and electrical properties of its based Schottky diodes. Optik, 164: 424–432.

29. Patterson AL (1939) The Scherrer formula for X-Ray particle size determination. Phys. Rev., 56: 978-982.

30. Reka Devi M, Saranya A, Pandiarajan J, Dharmaraja J, Prithivikumaran N, Jeyakumaran N (2018) Fabrication, spectral characterization, XRD and SEM studies on some organic acids doped polyaniline thin films on glass substrate. J. King Saud Uni. Sci., 1-4.

31. Manfridini A P, de A, Godoy G C D de, Santos L de A (2017) Structural characterization of plasma nitrided interstitial-free steel at different temperatures by SEM, XRD and Rietveld method. J. Mater. Res. Technol., 6(1): 65-70.

32. Ingo G M, Riccucci C, Pascucci M, Messina E, Giuliani C, Biocca P, Di Carlo G (2018) Combined use of FE-SEM+EDS, ToF-SIMS, XPS, XRD and OM for the study of ancient gilded artefacts. Appl. Surf. Sci., 446: 168-176.

33. Zhang P, Wang T, Zhang L, Wu D, Frost R L (2015) XRD, SEM and infrared study into the intercalation of sodium hexadecyl sulfate (SHS) into hydrocalumite. Spectrochim. Acta Part A, 151: 673–678.

34. Portillo H, Zuluaga M C, Ortega L A, Alonso-Olazabal A, Murelaga X, Martinez-Salcedo A (2018) XRD, SEM/EDX and micro-Raman spectroscopy for mineralogical and chemical characterization of iron slags from the Roman archaeological site of Forua (Biscay, North Spain). Microchem. J., 138: 246–254.

35. Pang H, Wang X, Zhang G, Chen H, Lv G, Yang S (2010) Characterization of diamond-like carbon films by SEM, XRD and Raman spectroscopy. Appl. Sur. Sci., 256(21):6403-6407.

36. Vastag G, Apostolov S, Matijević B, Assaleh F (2018) Multivariate assessment of azo dyes' biological activity parameters. J. Chromatogr. B, 1084: 141-149.

37. El-Sonbati A Z, Diab M A, El-Bindary A A, Morgan S M, Barakat A M (2016) Spectroscopic, geometrical structures, DNA and biological activity studies of azo rhodanine complexes. J. Mol. Liq., 224: 105-124.

38. Shridhar A H, Keshavayya J, Peethambar S K, Joy Hoskeri H (2016) Synthesis and biological activities of Bis alkyl 1, 3, 4-oxadiazole incorporated azo dye derivatives. Arabian J. Chem., 9: 1643-1648.

39. El-Sonbati A Z, Diab M A, El-Bindary A A, Shoair A F, Hussein M A El-Boz R A (2017) Spectroscopic, thermal, catalytic and biological studies of Cu(II) azo dye complexes. J. Mol. Struct., 1141: 186-203.

40. Khojasteh V, Kakanejadifard A, Zabardasti A, Azarbani F (2018) Spectral structural, solvatochromism, biological and computational investigation of some new azo-azomethines containing N-alkylpyridinium salts. J. Mol. Struct., 1175: 261-268.

